Front. Earth Sci. 2018, 12(4): 834–845
https://doi.org/10.1007/s11707-018-0730-z

RESEARCH ARTICLE

A study on flooding scenario simulation of future extreme precipitation in Shanghai

Xiaoting WANG, Zhan'e YIN (✉), Xuan WANG, Pengfei TIAN, Yonghua HUANG

Department of Geography, Shanghai Normal University, Shanghai 200234, China

Abstract In the context of climate warming and urbanization, predictions and inundation simulations for future extreme precipitation have become highly active research topics. In this paper, using daily precipitation recorded at 10 meteorological stations in Shanghai for the period 1961–2010, the daily precipitation of each station during the period 2011–2099 was simulated by the statistical downscaling model (SDSM). And we examined the varying tendencies of future precipitation by the Mann-Kendall test. Further, the Soil Conservation Service (SCS) model and Pearson-III distribution curve were used to simulate the waterlogging duration and depth of future extreme precipitation in different scenarios with 3-, 5-, 10-, 20-, 50-, and 100-year return periods. The results show that: 1) Precipitation in Shanghai before the 2050s shows a trend of increasing and decreasing alternations, followed by a trend of decreasing and a marked decrease in about the 2070s. 2) In the 21st century, the waterlogging duration with return periods of 3, 5, and 10 years in Shanghai is predicted to last for less than 30 minutes, while the return periods of 20, 50, and 100 years last for less than 45 minutes. From the spatial distribution, the waterlogging duration to the east and south of the Huangpu River is predicted to be shorter than that of the west and north. 3) With the increase of the return periods, the depth of waterlogging is predicted to increase. The deepest inundated areas are Jinshan to the south-west of Shanghai, the east side of the Huangpu River, and Chongming Island.

Keywords flooding scenario simulation, future extreme precipitation, Shanghai

1 Introduction

According to the Fifth Intergovernmental Panel on Climate Change (IPCC) Assessment Report on Climate Change, the intensity and frequency of extreme precipitation events may increase with global warming (IPCC, 2013). Therefore, research on extreme precipitation is widely regarded as an imperative focus of climate study, and it has aroused great concern in the international community and among scholars at home and abroad. Many scholars have studied threshold determinations, characteristics, mechanisms, and simulations of extreme precipitation. Numerous studies have focused on using detrended fluctuation analysis and the percentile method to define the extreme precipitation threshold (Lu et al., 2010; Zheng et al., 2012; Liu et al., 2013; Sukovich et al., 2014; Chi et al., 2016). Through observation data, many researchers have analyzed the historical variation characteristics and pointed out an increasing trend of extreme precipitation in China (Hang et al., 2003; Qian et al., 2007; Yuan et al., 2017). In the precipitation mechanism studies, Hu et al. (2003) proposed that the interdecadal variations in sea surface temperatures of the tropical Pacific and Indian Oceans affect China's summer precipitation through a subtropical high belt, and Tao and Wei (2007) pointed out that the anomalies of summer monsoons in East Asia have a significant impact on torrential rains in southern China. Based on the predictions of climate change scenarios provided by the CSIRO 9 model, Schreider et al. (2000) simulated the extreme precipitation in three regions of Australia. In addition, Li and Ding (2005) used regional climate models to simulate the East Asian monsoon and precipitation in China. The prediction results of global climate models with grid resolution of several hundred kilometres are often uncertain in urban scale research. To make up for these deficiencies, dynamic downscaling and statistical downscaling methods have been gradually applied to the research field to obtain more accurate precipitation prediction results. At present, the threshold determinations and long-term variation characteristics of extreme precipitation events are relatively clear, and there are many studies on the causes of their occurrence. However, based

Received March 31, 2018; accepted July 24, 2018

E-mail: zhaneyin@126.com

on the characteristics of precipitation variation, there are few studies on predicting future extreme precipitation by the statistical downscaling method, which then simulate urban waterlogging.

Shanghai is located in the mid-latitude region, and rainstorm waterlogging disasters are frequent (Liao et al., 2012; Zheng et al., 2012). From June 16 to 17, 2015, there were heavy rainstorms in Hongkou, Yangpu, Baoshan, Jiading, and other places in Shanghai, which caused a waterlogging depth of 10–20 cm in more than 20 sections of roads and 5–10 cm in more than 10 residential areas. On September 13, 2013, Shanghai suffered a torrential rain event representing a return period of 100 years. As a result, waterlogging depths for more than 80 roads in Pudong, Huangpu, Yangpu, Changming, and other central urban areas were 20–50 cm, causing serious damage to the urban transport system. On August 25, 2008, a short-term heavy rainfall in Shanghai caused a waterlogging depth of 10–60 cm in 170 road sections. In addition, more than 14,000 dwellings were flooded, and traffic in some parts of the downtown area was heavily congested. On August 6, 2005, torrential rains caused by typhoon "Matsa" flooded more than 200 roads and 50,000 households in Shanghai, with a direct economic loss of 1.358 billion CNY.

Based on data sets of daily precipitation recorded at 10 meteorological stations in Shanghai for the period of 1961–2010, this study applied a statistical model of local climate to the climatological information of the global climate model (GCM) and simulated daily precipitation data in Shanghai from 2011–2099. Using the Mann-Kendall test to analyse the trend of precipitation in the future, the SCS-CN hydrological model and Pearson-III distribution curve were used to simulate the waterlogging duration and depth of future extreme precipitation under different reoccurrence scenarios. The results provide a reference and basis for the urban government to carry out disaster prevention and mitigation of extreme precipitation.

2 Materials and methods

2.1 Study area

Shanghai is one of the coastal megacities in China, bordering the Jiangsu and Zhejiang provinces (Fig. 1). Shanghai has very flat and low-lying land, and the elevation is on average about four meters above the Wusong Datum. The total area of the municipality of Shanghai is 6340.5 km^2 (Shanghai

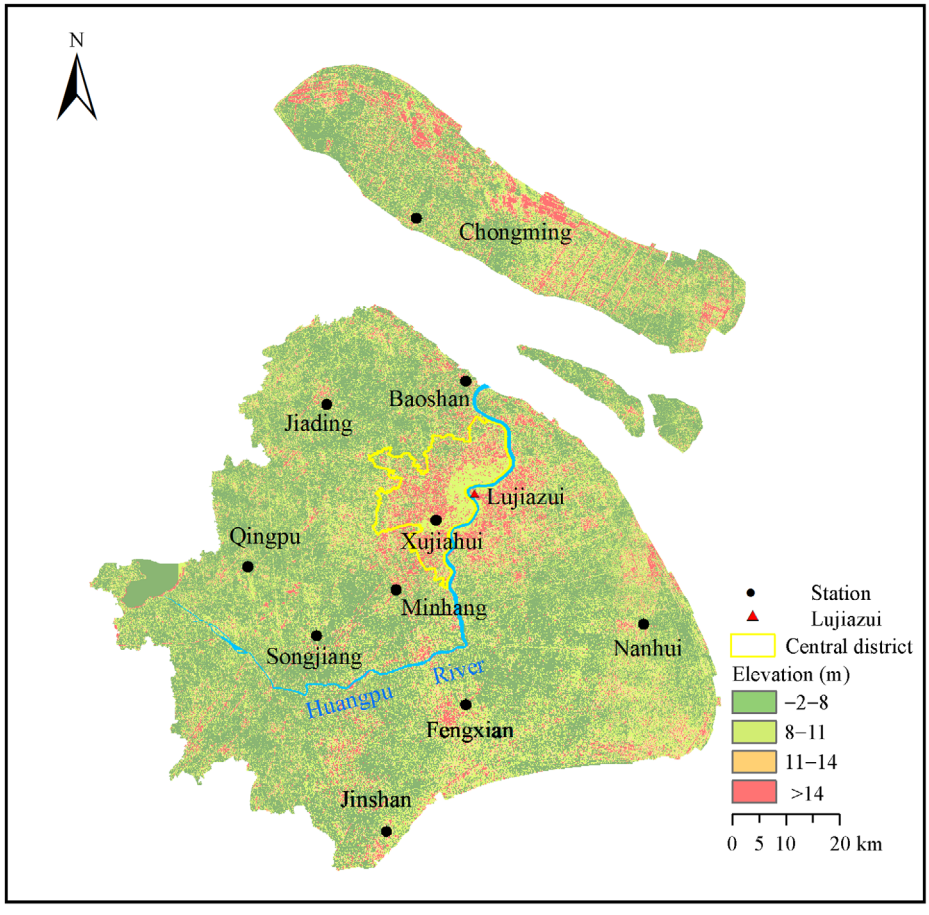

Fig. 1 The spatial distribution of 10 weather stations across Shanghai.

Municipal Statistics Bureau, 2015), and it has a population of 24.15 million (2015). Moreover, the city experiences a northern subtropical monsoon climate (Xu et al., 2004), with an annual rainfall of 1122 mm and an annual average temperature of 15.8°C. In the flood season, the frequency of extreme precipitation is high, and the spatial distribution of precipitation in the suburbs of Shanghai is quite different (Zhou and Yang, 2001; He et al., 2006). Shanghai is located in the lower reaches of the Yellow River basin and affected by the aging of the drainage network, low-lying terrain, and tidal topping, all of which have caused more frequent extreme precipitation events, which have resulted in flood disasters of great impact (Chen et al., 2014; Gao and Xie, 2016; Yin et al., 2016; Guan et al., 2017).

2.2 Data

The research data includes data for precipitation, basic geography, drainage, and climate models. The precipitation data comes from daily precipitation at 10 local meteorological stations in Shanghai over the period 1961–2010 provided by the Shanghai Meteorological Bureau, for which the accuracy is 0.1 mm. The basic geographic data includes land use data for 2006 with a spatial resolution of 1 m from the Key Laboratory of Geographic Information Science of East China Normal University and administrative division data from the National Basic Geographic Information Center. The drainage data comes from the Shanghai Drainage Strategic Plan for 2020 provided by the Shanghai Drainage Management Office. The climate model data includes National Centers for Environmental Prediction (NCEP) reanalysis data from the US Environmental Prediction Center and the National Center for Atmospheric Research as well as GCM Atmospheric Circulation data from the Hadley Centre for Climate Prediction and Research in the UK.

2.3 Methods

2.3.1 Future precipitation forecasting method

The future precipitation prediction uses the statistical downscaling model (SDSM), which predicts climatic change based on long-term statistical monitoring data. It is widely used in the simulation and remedial decision making of rainstorms in urban areas around the world (Brown and Wilby, 2012; Wilby and Dawson, 2013). After forecasting factor screening, parameter calibration, and model validation, a model is established to simulate the precipitation in future scenarios. The model is a downscaling model of climate change recommended by the IPCC and developed by Rob Wilby of Loughborough University in the UK. The principle is to establish a statistical relationship between global climate elements and local forecasts through multi-year observations at weather stations. The established relationship is verified and the model assumes that the relationship will remain valid in the future. Thus the local climate statistical relationship is applied to the climate information output from the GCM to predict local climate change scenarios in the future.

Our global circulation model used 1961–2099 data from the Hadley Centre's HadCM3 GCM in the A2 scenario, and the NCEP reanalysis data was converted by the CCIS (making it the same resolution as the HadCM3). Using the NCEP reanalysis data and daily precipitation data from 1961–2010 to establish and test the downscaling model of precipitation in Shanghai, the data of the first 30 years (1961–1990) was used to establish the model, and the data from 1991–2010 was used to test. Then the data of 1961–2099 simulated by HadCM3 in the A2 scenario was used to predict the future precipitation.

At the same time, using the Mann-Kendall (MK) test, we conducted a mutation analysis on the precipitation in various scenarios in the future, and identified the precipitation characteristics. The mutation testing method is recommended by the World Meteorological Organization to judge whether the development of the sequence represents an upward or a downward trend (Fu and Wang, 1992). In the result, if the value of UF or UB is greater than 0, the sequence shows an upward trend, while a value of less than 0 indicates a downward trend. When a value is above the critical line, it shows a significant upward or downward trend. If the UF and UB curves appear intersection point and it is between the critical lines, the intersection point corresponding moment is the start of the jump time.

2.3.2 Inundation simulation method

Under different scenarios, drainage capacity and surface run-off are two key factors in inundation simulation. The Shanghai Drainage Strategic Plan for 2020 (Shanghai Municipal Drainage Administration, 2007) was selected as the drainage capacity value. In planning, Shanghai is divided into 15 drainage areas. Among them, the drainage capacity of Yunan Pian, Dianbei Pian, and downtown areas is higher than that of other areas, with drainage capacity of about 1 $m^3/s/km^2$, basically reaching the standard of a 20-year return period. Surface run-off used the SCS model proposed by the American Soil Conservation Service, which is widely used at home and abroad (Novotny et al., 1981; McCuen, 1982). Run-off was calculated from the empirical run-off coefficients of different underlying surfaces in Shanghai. And the depth of run-off can be calculated as follows:

$$Q = \left((P-0.2S)^2/(P+0.8S)\right)(P \geqslant 0.2S)$$

$$\text{or } 0(P < 0.2S), \quad (1)$$

$$S = 25400/C_{CN} - 254, \quad (2)$$

where Q is run-off depth (mm), P is the total amount of rainfall (mm), S is the maximum possible retention (mm) during the precipitation, and C_{CN} (Curve Number) is a comprehensive parameter that reflects the characteristics of the basin; its values are listed in Table 1 (Quan et al., 2009).

Table 1 CN values in SCS model

Land type	Curve number
Water	100
Park	70
Forestland	57
Green space	62
Unused land	83
Natural village	76
Old residential	92
Cultivated land	78
Public building	88
Warehouse land	89
New residential	86
Roads and squares	98
Commercial and industrial	93

2.3.3 Future inundation scenario design

For the future inundation analysis, the MK test shows that the abrupt period of total precipitation is predicted for the 2050s to the 2070s. To make a detailed analysis, it is necessary to select one year of the abrupt period as the dividing point. Therefore, the 2050s was selected to divide the period of predicting precipitation in the future (2011–2099), encompassing both the first half (2011–2050) and the second half (2051–2099) of the 21st century. Then, using the frequency analysis method of Pearson-III distribution (Zhu and Wang, 2006; Xu et al., 2007), annual maximum sampling was used to calculate the extreme values with return periods in the study area. Finally, based on the urban run-off model and drainage capacity, six extreme precipitation scenarios of 3-, 5-, 10-, 20-, 50-, and 100-year return periods were designed to dynamically simulate the inundation from urban extreme precipitation. The probability distribution function of Pearson-III is as follows:

$$\alpha = \frac{4}{C_S^2},\ \beta = \frac{2}{\overline{X} C_V C_S},\ a_0 = \overline{X}\left(1 - \frac{2C_V}{C_S}\right),$$

$$F(x) = P(X \geqslant x) = \int_x^{+\infty} \frac{\beta^\alpha}{\tau(\alpha)} (x - a_0)^{\alpha-1} e^{-\beta(x-a_0)} dx, \quad (3)$$

where C_V and C_S is the coefficient of variation, $\overline{X}$ is the average, and α, β, and a_0 are the parameters to be fitted for the Pearson-III distributions and can be determined by the curve-fitting method (SL44, 1993).

3 Results and discussion

3.1 Forecast and variation characteristics of future precipitation

Based on the daily precipitation data of 10 local weather stations in Shanghai from 1961 to 2000, followed by the four major criteria for the selection of forecasting factors (Fan et al., 2005), the "variable screening" module in the SDSM model was used to select the forecast factor. By means of partial correlation analysis and scatter plot fitting, we determined the four forecast factors that were suitable for precipitation forecasts at each site (Table 2).

Table 2 Predictor screening results

Forecast volume	Forecast factor
Precipitation	r500 (relative humidity at 500 hPa)
	r850 (relative humidity at 850 hPa)
	p8_v (convective velocity at 850 hPa)
	p8_z (vortices at 850 hPa)

Using the daily precipitation data from 1961 to 1990 at each site and the selected forecast factors, a regression model was established with quadratic roots in 12 months, and the daily average precipitation data from 1991 to 2010 was used to verify the results. The assessment of climate model predictions generally uses correlation coefficients or the root-mean-square error to verify proximity to actual observations (Tao et al., 2012). In this study, the correlation coefficient was used to verify the accuracy of the model. Under the 95% confidence level, the correlation coefficient of each station (Table 3) was obtained, and the value was high. So the simulation accuracy of the model is high and the result is credible.

Table 3 Coefficient of association (SDSM)

Precipitation station	Correlation coefficient (r)
Xujiahui	0.68
Minhang	0.71
Baoshan	0.72
Jiading	0.75
Chongming	0.77
Nanhui	0.79
Jinshan	0.74
Qingpu	0.73
Songjiang	0.74
Fengxian	0.71

The autocorrelation coefficients of the future precipitation data of the 10 sites were all less than 0.1, the time series were independent, and the MK test can be used directly. Taking the confidence level of 0.05 (the critical value of 1.96), the mutation test was conducted by the MK test. The abrupt shifts of total annual precipitation in the future scenario of each year (2011–2099) were calculated (Fig. 2). The UF statistic values in Shanghai's southeastern coastal areas, such as Nanhui and Jinshan, increase until the 2060s, indicating that the annual precipitation in these areas has an ascending trend, and then the UF curve starts to decline and intersects with the UB statistical curve around the 2070s, suggesting a significant decrease in total precipitation in the 2070s. The annual precipitation in other

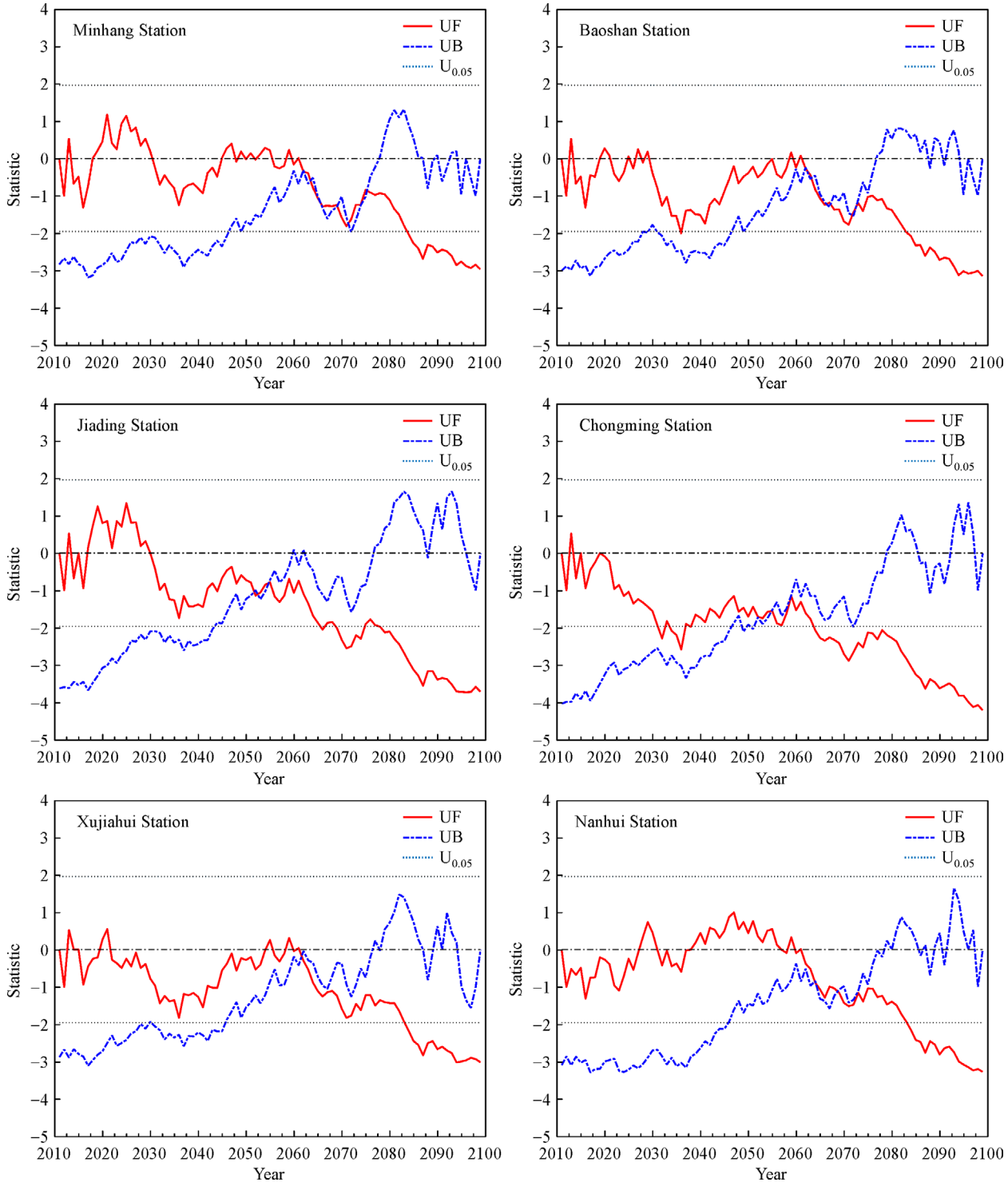

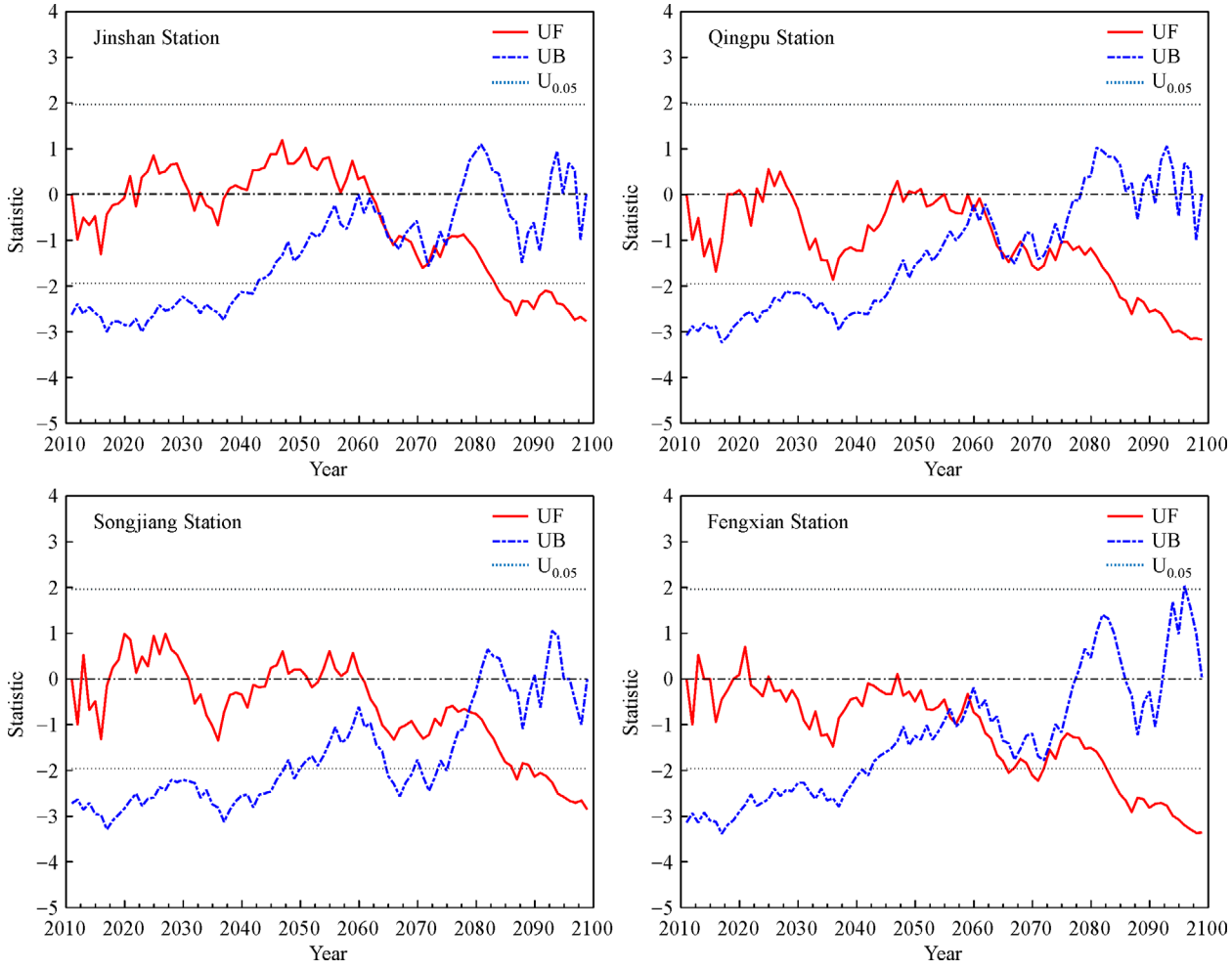

Fig. 2 Trend analysis of future precipitation amounts.

parts of Shanghai tends to increase and decrease alternately before the 2050s. The UF is less than 0 and the intersection of the UF and UB curves shows that there is a sudden drop of precipitation in these areas around the 2060s. In general, a sudden drop in total precipitation occurs in various regions of Shanghai between the 2050s and the 2070s.

3.2 Inundation scenario simulation in the first half of the 21st century

3.2.1 Waterlogging duration in different scenarios

Based on the SDSM model, the maximum single-day precipitation values were simulated. Taking the return periods of 3, 5, 10, 20, 50, and 100 years as different scenarios, the extreme precipitation in each scenario was obtained by using the Pearson-III frequency distribution curve. The SCS-CN empirical hydrological model was constructed under the ArcGIS software platform to get the surface run-off at different return periods. And taking the drainage capacity of the Shanghai Drainage Strategic Plan for 2020 (Shanghai Municipal Drainage Administration, 2007) as a reference, we simulated the waterlogging duration (Fig. 3) and depth (Fig. 4) in each scenario of the first half of the 21st century.

In terms of the waterlogging duration, for the 3-, 5-, and 10-year return periods the duration does not last more than 30 minutes, and for the 20-, 50-, and 100-year return periods it does not last more than 45 minutes. From the perspective of spatial distribution, the Huangpu River is the boundary in different scenarios, and the waterlogging duration in the east and south areas of the Huangpu River is generally greater than that in the west and north areas of the river. In addition, on Chongming Island, with the increase of return period, the waterlogging duration from the north-west to the south-east gradually increases. During the return period of 3 years, waterlogging for most areas of Shanghai lasts less than 20 minutes, and the areas with longer duration are concentrated in Chongming Island, Pudong, and Fengxian. The central urban areas to the west

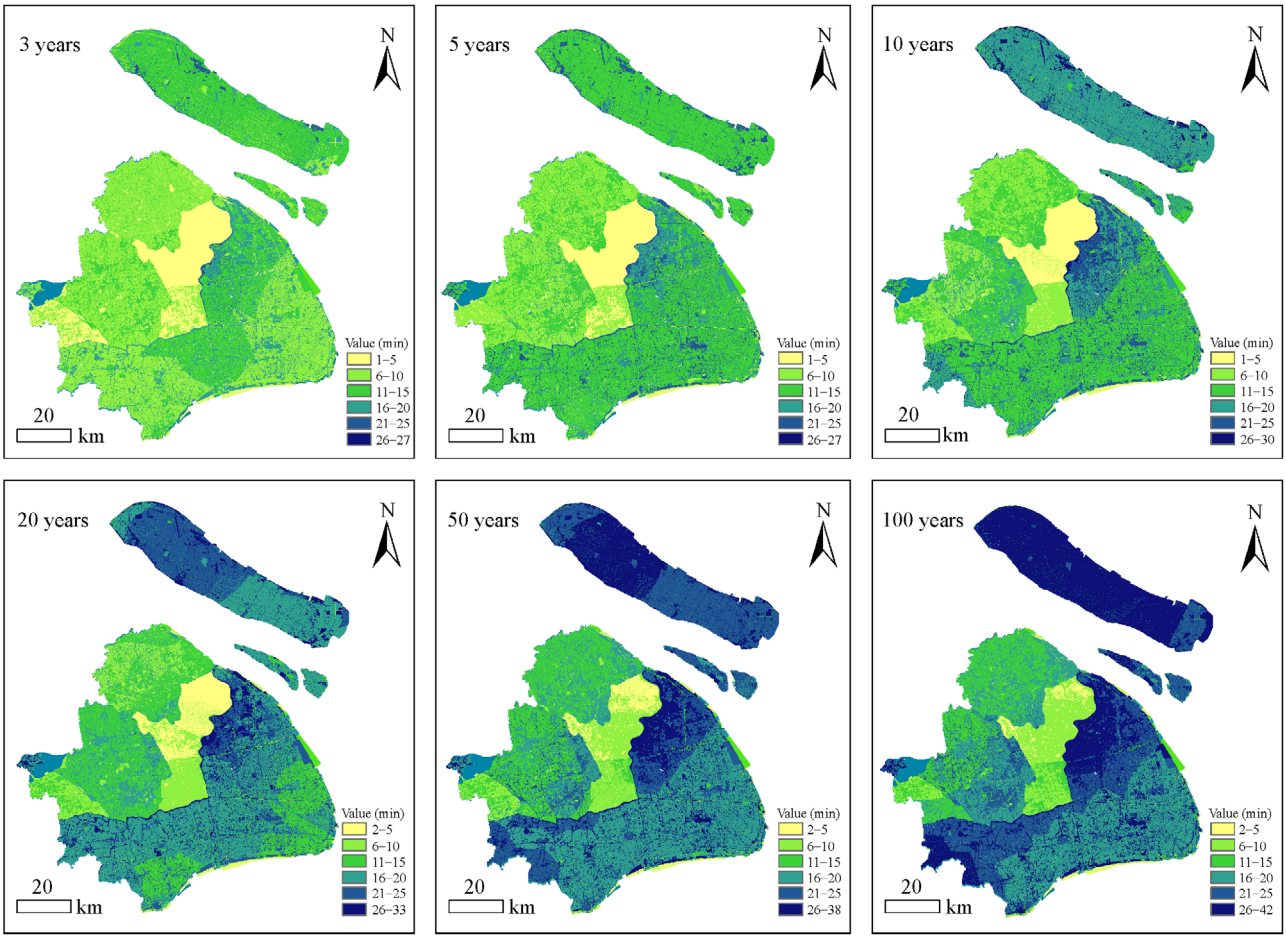

Fig. 3 Waterlogging duration in the first half of the 21st century under different return periods.

of the Huangpu River last the shortest time, less than 5 minutes. During the return period of 5 years, the duration in the east and south areas of the Huangpu River and Chongming Island is the longest, increasing to about 20 minutes. And the waterlogging duration in the west and north of the Huangpu River is less than 10 minutes. During the return period of 10 years, the spatial range of the areas with longer duration increases significantly, and the longest waterlogging duration is in Lujiazui, which is about 30 minutes. During the return period of 20 years, the duration of waterlogging in Shanghai increases to about 33 minutes, and the duration in the north-east of Chongming Island lasts for about 25 minutes. During the return period of 50 years, the waterlogging duration in the east and south areas of the Huangpu River increases drastically over 25 minutes. And the duration in the north-east of Chongming Island lasts over 38 minutes. During the return period of 100 years, the waterlogging duration in Shanghai increases to 42 minutes, and it increases on Chongming Island from north-west to south-east. The duration in the downtown area increases to about 10 minutes.

3.2.2 Waterlogging depth in different scenarios

In contrast to the return periods of 3, 5, 10, and 20 years, the calculation of the waterlogging depth during the return periods of 50 and 100 years is based on the fact that the waterlogging duration of the two periods is longer and the precipitation amount is larger. It can fully reflect the complex inundation situation in Shanghai. In particular, simulating the heavy rain under the recurrence periods of 50 and 100 years can provide the basis for disaster prevention and mitigation in advance for heavy rainstorms in Shanghai.

In the first half of the 21st century, the depth of waterlogging was obtained under the 15-minute and 30-minute durations for the two return periods of 50 and 100 years, based on the ArcGIS platform (Fig. 4). With the increase of the recurrence period, the waterlogging depth of Shanghai increases. The waterlogging depth increases to 163 mm and 73 mm for 15 minutes and 30 minutes, respectively, of the period of 100 years. The areas with the largest waterlogging depth are Jinshan District in the

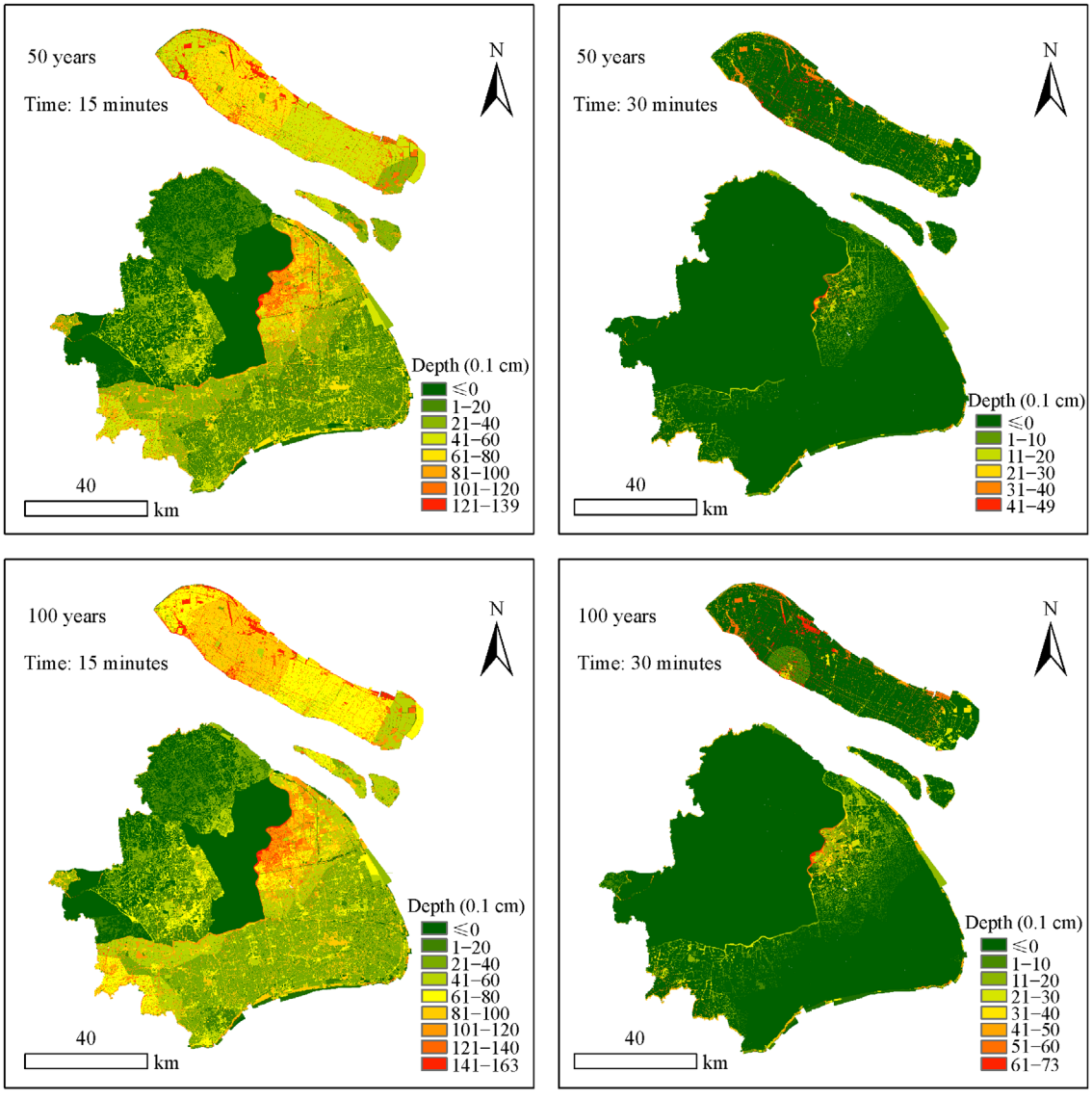

Fig. 4 Waterlogging depth in the first half of the 21st century under different return periods (left 15 minutes, right 30 minutes).

south-west of Shanghai, the east side of the Huangpu River, and Chongming Island. At 15 minutes in the first half of the 21st century, the maximum depth is about 140 mm in the 50-year return period and 160 mm in the 100-year return period. At 30 minutes, the waterlogging depth gradually decreases with time. The maximum depth is reduced to 50 mm in the 50-year return period and 70 mm in the 100-year return period. From the spatial distribution, the maximum waterlogging depth at 15 minutes with the 50-year return period is located in Chongming Island and the east side of the Huangpu River. Furthermore, the depth in the north-west of Chongming Island clearly increases. At 30 minutes with the 50-year return period, the waterlogging areas include Jinshan District, Chongming Island, and the east side of the Huangpu River. At 30 minutes with the 100-year return period, the waterlogging areas on the east side of the Huangpu River and Chongming Island further expand.

3.3 Inundation scenario simulation in the second half of the 21st century

3.3.1 Waterlogging duration in different scenarios

On the ArcGIS platform, the waterlogging duration (Fig. 5) and depth (Fig. 6) were obtained for each scenario in the second half of the 21st century by using the future inundation scenario design and simulation method. The waterlogging duration for the first half of the 21st century is similar to that of the second half of the 21st century. For example, the waterlogging duration does not last more than 30 minutes in the 3-, 5-, and 10-year return periods and 45

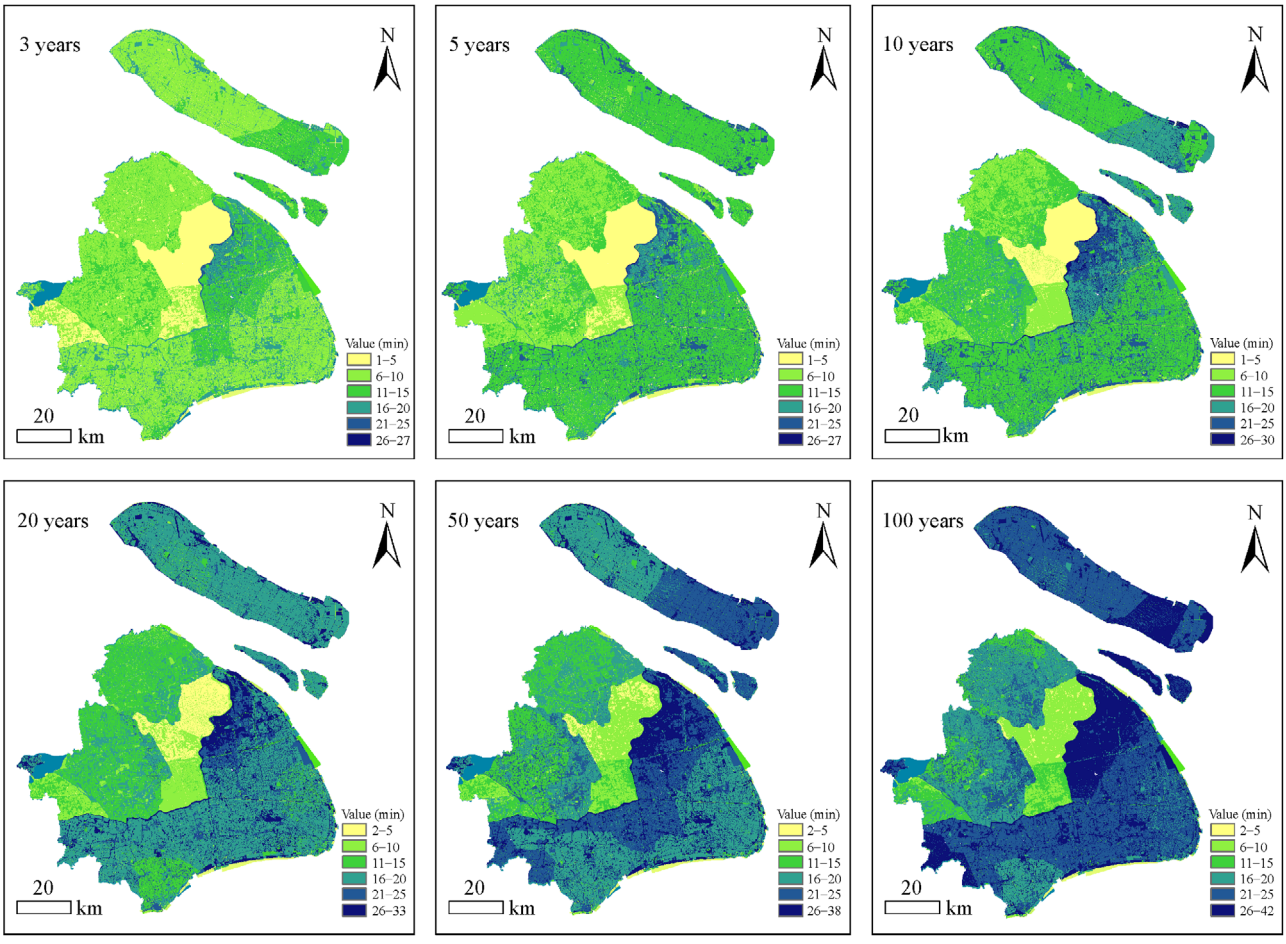

Fig. 5 Waterlogging duration in the second half of the 21st century under different return periods.

minutes in the 20-, 50-, and 100-year return periods. Huangpu River is the boundary in the different scenarios, and the waterlogging durations in the east and south areas of the Huangpu River are generally greater than those in the west and north areas of the river. However, in the second half of the 21st century, the waterlogging duration in the south-east of Chongming Island is longer than that in the north-west, and the waterlogging duration on the island as a whole is less than that during the first half of the century. In addition, the ranges for waterlogging durations lasting more than 15 minutes continuously expand in the mainland area of Shanghai. For example, in the return period of 5 years, the waterlogging areas expand from Lujiazui to the east of the Huangpu River in the north coastal zone; in the return periods of 20 years and 100 years, the areas from the east and the south of the Huangpu River are expanded to the boundaries of Jinshan, Fengxian, and Nanhui of Shanghai.

3.3.2 Waterlogging depth in different scenarios

Through comparing the first half and the second half of the 21st century, the maximum depth of waterlogging in 15 minutes and 30 minutes is similar under the two return periods of 50 and 100 years (Fig. 6). The drainage capacity value used for this study is the design value of the Shanghai Drainage Strategic Plan for 2020. Under the drainage conditions planned and designed, the waterlogging duration of extreme precipitation in Shanghai in 50 years is 10–38 minutes, and that in 100 years is 10–42 minutes. Thus when the water in most parts of Shanghai is basically exhausted in 30 minutes, the waterlogging depth in 30 minutes is less than 15 minutes in the first half and the second half of the 21st century. However, in the second half of the 21st century, the waterlogging depth at 15 minutes and 30 minutes is more concentrated, and the areas with the higher level of waterlogging are larger. And the waterlogging depth in the first half of the 21st century on Chongming Island is smaller than that in the second half of the century. With the 15-minute duration in the second half of the 21th century, the maximum waterlogging depth is about 140 mm in the 50-year return period and 160 mm in the 100-year return period. At 30 minutes, the maximum depths of waterlogging in the 50- and 100-year return periods are about 50 mm and 70 mm, respectively. Spatially, compared with the 15 minutes of the first half

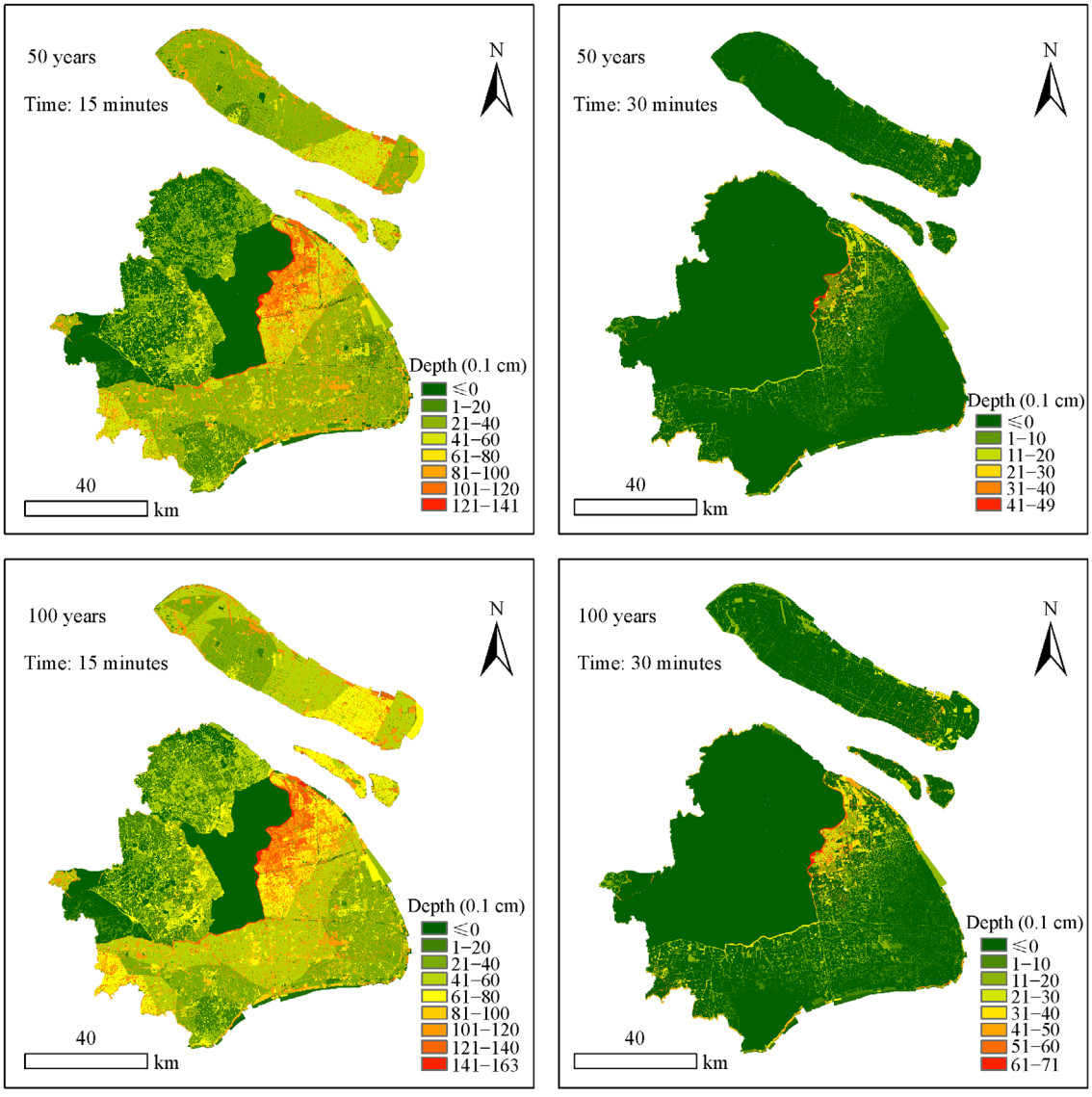

Fig. 6 Waterlogging depth in the second half of the 21st century under different return periods (left 15 minutes, right 30 minutes).

of the 21st century, the distribution range of the waterlogging depth above 40 mm significantly expands in the Shanghai urban area, while the area of Chongming Island below the waterlogging depth of 40 mm is significantly reduced. At 30 minutes, the spatial area above 20 mm in waterlogging depth is significantly enlarged in the mainland area of Shanghai. The distribution range of Chongming Island below 20 mm in waterlogging depth is significantly reduced.

4 Discussion and conclusions

Taking Shanghai as the case study, this paper uses the SDSM model and the MK test method to obtain predictions for future precipitation and its change characteristics. Then, based on the simulated daily precipitation in the period 2011–2099, the SCS model and Pearson-III frequency analysis method are used to obtain the waterlogging duration and depth with 3-, 5-, 10-, 20-, 50-, and 100-year return periods. The main conclusions are as follows:

1) Based on the MK test, the future total precipitation in the south-eastern coastal areas of Shanghai, such as Nanhui and Jinshan, shows a decreasing mutation around the 2070s, and the mutation is significant; the total precipitation significantly reduces in other urban areas of Shanghai around the 2060s, after which the total precipitation decreases.

2) In the first and second halves of the 21st century, waterlogging for the 3-, 5-, and 10-year return periods does not last more than 30 minutes, and for the 20-, 50-, and 100-year return periods it does not last more than 45 minutes. From the perspective of spatial distribution, the

Huangpu River is the boundary in different scenarios, and the waterlogging durations in the east and south areas of the Huangpu River are generally greater than those in the west and north areas of the river. On Chongming Island, with the increase of the return periods, the waterlogging duration decreases; in the mainland area of Shanghai, the ranges for waterlogging duration lasting 15 minutes constantly expand.

3) In the first and second halves of the 21st century, the depth of waterlogging increases with the increase of return period. The areas with the maximum inundation depth are the Jinshan District in south-western Shanghai, along the east side of the Huangpu River, and Chongming Island. The maximum depth of waterlogging is about 140 mm in the 50-year return period and 160 mm in the 100-year return period. Compared with the first half of the 21st century, the waterlogging depth of the mainland area in Shanghai is greater, and the inundation depth of Chongming Island is smaller.

In this study, long-term daily precipitation data from a series of meteorological stations was used to solve the problem of insufficient precision in urban precipitation research. The downscaling model of climate statistics was introduced from the watershed area to the urban area, and the trend for precipitation in Shanghai was predicted more accurately. At the same time, extreme precipitation inundation scenarios were simulated from temporal dynamics. However, further improvements are recommended for this type of research. For example, the statistical downscaling method was used for the future precipitation prediction, which is limited to the accuracy of the climate model. In the future, we can consider combining dynamic downscaling methods to produce predictions. In addition to using the stationary assumption and Pearson-III, there are other methods such as non-stationarity, GEV, and GPD. To improve the extreme precipitation accuracy of the analysis, the next step could be a comparative study of these methods. There are many natural and human factors that affect climate change in combination, and these need further study. Especially when calculating the depth of urban waterlogging, combined with the current status of land use change caused by urbanization in Shanghai, different run-off models could be selected according to land use types or different drainage areas.

Acknowledgements The work was supported by the National Natural Science Foundation of China (Grant Nos. 41371493 and 41071324), and the Innovation Program of the Shanghai Municipal Education Commission (13YZ061).

References

Brown C, Wilby R L (2012). An alternate approach to assessing climate risks. Eos (Wash DC), 93(41): 401–402

Chen Y D, Zhang Q, Xiao M Z, Singh V P, Leung Y, Jiang L G (2014). Precipitation extremes in the Yangtze River Basin, China: regional frequency and spatial–temporal patterns. Theor Appl Climatol, 116 (3–4): 447–461

Chi X X, Yin Z E, Wang X, Sun Y K (2016). Spatiotemporal variations of precipitation extremes of China during the past 50 years (1960–2009). Theor Appl Climatol, 124(3–4): 555–564

Fan L J, Fu C B, Chen D L (2005). Review on creating future climate change scenarios by statistical downscaling techniques. Advances in Earth Science, 20(3): 320–329 (in Chinese)

Fu C B, Wang Q (1992). The definition and detection of the abrupt climatic change. Chin J Atmos Sci, 16(4): 482–493

Gao T, Xie L (2016). Spatiotemporal changes in precipitation extremes over Yangtze River Basin, China, considering the rainfall shift in the late 1970s. Global Planet Change, 147: 106–124

Guan Y H, Zheng F L, Zhang X C, Wang B (2017). Trends and variability of daily precipitation and extremes during 1960–2012 in the Yangtze River Basin, China. Int J Climatol, 37(3): 1282–1298

Hang R H, Chen J L, Zhou L T, Zhang Q Y (2003). Studies on the relationship between the severe climatic disasters in China and the East Asia climate system. Chin J Atmos Sci, 27(4): 770–787

He F F, Gu X D, Xu J L (2006). Studies on radiation resource change in Shanghai since the 1990s. Journal of Natural Resources, 20(2): 210–216 (in Chinese)

Hu Z, Yang S, Wu R (2003). Long-term climate variations in China and global warming signals. J Geophys Res D Atmospheres, 108(D19): 4614

IPCC (2013). Climate Change 2013: The Physical Science Basis. Cambridge University Press

Li Q P, Ding Y H (2005). Multi-year simulation of the East Asian monsoon and precipitation in China using a regional climate model and evaluation. Acta Meteorol Sin, 19(3): 302–316

Liao Y F, Nie C J, Yang L S, Li H R (2012). An overview of the risk assessment of flood disaster. Progress in Geography, 31(3): 361–367 (in Chinese)

Liu B J, Chen J F, Chen X H, Lian Y Q, Wu L L (2013). Uncertainty in determining extreme precipitation thresholds. J Hydrol (Amst), 503 (11): 233–245

Lu H, He H, Chen S R (2010). Spatiotemporal variation of extreme precipitation frequency in summer over South China in 1961–2008. Journal of Ecology, 29(6): 1213–1220 (in Chinese)

McCuen R H (1982). A Guide to Hydrologic Analysis Using SCS Method. Englewood Cliffs: Prentice-Hall

Novotny V, Chesters G, Shannon J (1981). Handbook of Non-Point Pollution Source and Management. New York: Van Nostrand Reinhold Company

Qian W H, Fu J L, Zhang W W, Lin X (2007). Changes in mean climate and extreme climate in China during the last 40 years. Advances in Earth Science, 22(7): 673–683 (in Chinese)

Quan R S, Liu M, Hou L J, Lu M, Zhang L J, Ou D N, Xu S Y, Yu L Z (2009). Impact of land use dynamic change on surface runoff: a case study on Shanghai Pudong new district. Journal of Catastrophology, 24(1): 44–49 (in Chinese)

Schreider S Y, Smith D I, Jakeman A J (2000). Climate change impacts on urban flooding. Clim Change, 47(1–2): 91–115

Shanghai Municipal Drainage Administration (2007). Shanghai urban

rainwater system professional planning. http://www.smda.org.cn/fore/Detail.aspx?id = 4802/ (accessed 16 August 2017)

Shanghai Municipal Statistics Bureau (2015). Shanghai Statistical Yearbook 2015. Beijing: China Statistics Press (in Chinese)

SL44 (1993). Design flood code for water conservancy and hydropower projects. https://wenku.baidu.com/view/e1895cd4b14e852458fb575e.html/ (accessed 26 June 2017)

Sukovich E M, Ralph F M, Barthold F E, Reynolds D W, Novak D R (2014). Extreme quantitative precipitation forecast performance at the weather prediction center from 2001 to 2011. Weather Forecast, 29(4): 894–911

Tao H, Bai Y G, Mao W Y (2012). Assessment of CMIP3 climate models and projected climate changes in northern Xinjiang. Geogr Res, 31(4): 589–596

Tao S Y, Wei J (2007). Correlation between monsoon surge and heavy rainfall causing flash-flood in southern China in summer. Meteorol Monogr, 33(3): 10–18

Wilby R L, Dawson C W (2013). The statistical down scaling model (SDSM): insights from one decade of application. Int J Climatol, 33 (7): 1707–1719

Xu L J, Li J Q, Li T, Liu X H (2007). On rainstorm intensity formula during little time in Shanghai. China Municipal Engineering, 4: 46–48

Xu S Y, Su J, Wang Z, Liu M, Zhang Z L, Wu J P, Huang Y M, Shi C, Lu L H (2004). Atlas of Shanghai urban physical geography. Shanghai: Chinese Map Publishing House (in Chinese)

Yin J, Yu D P, Wilby R (2016). Modelling the impact of land subsidence on urban pluvial flooding: a case study of downtown Shanghai, China. Sci Total Environ, 544: 744–753

Yuan Z, Yang Z Y, Yan D H, Yin J (2017). Historical changes and future projection of extreme precipitation in China. Theor Appl Climatol, 127(1–2): 393–407

Zheng T F, Guo J M, Yin J F, Wang Q, Wu W (2012). DFA-based research on spatiotemporal distribution of extreme precipitations in Jiangsu Province. Journal of Natural Disaster, 21(4): 76–83 (in Chinese)

Zhou L Y, Yang K (2001). Variation of precipitation in Shanghai during the last one hundred years and precipitation differences between city and suburb. Acta Geogr Sin, 56(4): 467–476

Zhu Y Y, Wang Y (2006). Frequency distribution statistical test of urban short-duration rainstorm in Fujian Province. Journal of Fuzhou University (Natural Science Edition), 34(3): 415–419 (in Chinese)